

Bidirectional reflectance of dry and submerged Labsphere Spectralon plaque

Kenneth J. Voss and Hao Zhang

We present the bidirectional reflectance of a Labsphere calibration plaque, both dry and submerged in water, at normal illumination. The measurements indicate that when submerged in water, the Labsphere calibration plaque has a higher reflectance value than when dry at viewing angles below 55° . The results are presented in the form of a reflectance factor and are useful for calibrating underwater reflectance measurements. © 2006 Optical Society of America

OCIS codes: 010.4450, 120.4800, 120.0280, 120.5700, 290.4210, 0.30.5620.

1. Introduction

In many remote sensing applications the measured bidirectional reflectance distribution function (BRDF) is calibrated with Spectralon diffuse reflectance standards (Labsphere, Eastern Regional Sales, North Sutton, New Hampshire) because of their near-Lambertian behavior at near-normal illuminations. However, as found by several research groups,¹⁻³ Spectralon plaques have significant deviations from a perfect diffuser in many aspects, and thus the BRDF of the plaque is often needed to correct for non-Lambertian effects. In recent years we have made BRDF measurements on various dry, water wetted, and underwater benthic sediment surfaces to study the effects of the particle physical properties on the BRDF. To calibrate the instrument and to measure the underwater sediment BRDF, an accurate BRDF of both a dry and a submerged Spectralon plaque is needed. Upon changing the scattering medium from air to water, the Spectralon BRDF may change significantly. In this paper we present goniometric scattering measurements of a Spectralon plaque, both dry and submerged, which may be used as benchmarks in underwater remote sensing applications.

2. Measurement and Result

The goniometer used in this work is an improved version of the one described in an earlier work,⁴ with modifications to improve the angular resolution. In this system, light from a He-Ne laser is inserted into an Edmund multimode FC fiber through a focus assembly. The multimode fiber is used to depolarize the laser light (and has been found to reduce the degree of polarization to less than 1%). After exiting the fiber the light is collimated by a lens and illuminates a 7 mm diameter region of the sample surface, when incident normal to the surface. The viewing optics consist of a focusing lens, an interference filter, which selects only the laser light, and a silicone photodiode. These optics are configured to view a 7 cm diameter area on the surface. The angular resolution is 0.7° full angle. To increase the signal-to-noise ratio we chop the incident laser beam, and the received signal is processed by a Stanford Research SR 830 lock-in amplifier before it is digitized by a National Instrument Data Acquisition-700 Personal Computer Memory Card International Association (PCMCIA) card (National Instruments) in a laptop computer. With this goniometer we use normal illumination and measure viewing angles from 15° to 70° and -70° to -19° in the principal plane, which is the plane containing the incident, viewing, and sample surface normal directions.

We use the reflectance factor⁵ (REFF) to describe the angular pattern of plaque reflectance as it gives the direct comparison to a perfect Lambertian reflector. The REFF is the ratio of the bidirectional reflectance of the sample, r_s , to that of a perfect Lambertian reflector, r_L ,

The authors are with the Department of Physics, University of Miami, Miami, Florida 33124. K. J. Voss's e-mail address is voss@physics.miami.edu.

Received 3 May 2006; revised 5 June 2006; accepted 11 June 2006; posted 13 June 2006 (Doc. ID 70589).

0003-6935/06/307924-04\$15.00/0

© 2006 Optical Society of America

$$\text{REFF}(\theta_i, \phi_i; \theta_v, \phi_v) = \frac{r_S(\theta_i, \phi_i; \theta_v, \phi_v)}{r_L} \quad (1)$$

$$\equiv \frac{r_S(\theta_i, \phi_i; \theta_v, \phi_v)}{\mu_0/\pi},$$

where μ_0 is the cosine of incident zenith angle, θ_i ; θ_v is the viewing zenith; ϕ_i and ϕ_v are the incident and viewing azimuth angles, respectively; and $r_{S,L}(\theta_i, \phi_i; \theta_v, \phi_v)$ are the bidirectional reflectances defined as the ratio of the radiance reflected by a surface in a given direction, L_r , to the collimated irradiance on the surface, E_i :

$$r(\theta_i, \phi_i; \theta_v, \phi_v) = \frac{L_r(\theta_v, \phi_v)}{E_i(\theta_i, \phi_i)}. \quad (2)$$

Since in this work the measurements are taken in the principal plane under normal illumination, both the REFF and r are dependent only on θ_v . Our sample is a 2 in. diameter Labsphere Spectralon plaque SRS-99-020 (serial no. 45204-1-1) manufactured in April 2005. At an 8° incident angle, the REFF of this plaque measured by our goniometer agrees with the published data² within 1% over viewing zenith angles from 0° to 55° and is 4% lower at 70° . To measure the REFF of a plaque submerged in water, a cylindrical 20 cm diameter glass jar is used as the container.⁶ First, measurements were done with the plaque in air; then the cylindrical jar was installed and the plaque was measured again. We then filled the jar with pure water (HPLC Grade, J. T. Baker CAS 7732-18-5) and the submerged reflectance was measured. Care was taken to ensure that no bubbles were present on the plaque surface during the measurements. To obtain the submerged REFF, the following procedures were employed to correct for the air–glass and glass–water interface effects.

The radiances reflected from the plaque without the jar in place (“bare”), dry but in the glass jar (“jar”), and in the water-filled glass jar (“sub”) may be described as

$$E_i r^{\text{bare}} = L^{\text{bare}}, \quad (3)$$

$$E_i t_{\text{ag}} t_{\text{ga}} r^{\text{bare}} t_{\text{ag}} t_{\text{ga}} = L^{\text{jar}}, \quad (4)$$

$$E_i T_{\text{abs}} t_{\text{ag}} t_{\text{gw}} \frac{r^{\text{sub}}}{n} t_{\text{wg}} t_{\text{ga}} = L^{\text{sub}}, \quad (5)$$

where $t_{\text{ag}} (= t_{\text{ga}})$ and $t_{\text{gw}} (= t_{\text{wg}})$ are Fresnel transmission coefficients of air–glass (glass–air) and glass–water (water–glass) interfaces, respectively; T_{abs} is the transmission loss over the 20-cm-long path length in water and n is the refractive index of water. This refractive index correction was applied because of the cylindrical geometry of our glass jar (see Appendix A). Since the incident irradiance could not be measured directly with our apparatus, we used the following relationship to obtain the bare plaque $\text{REFF}^{\text{bare}}$:

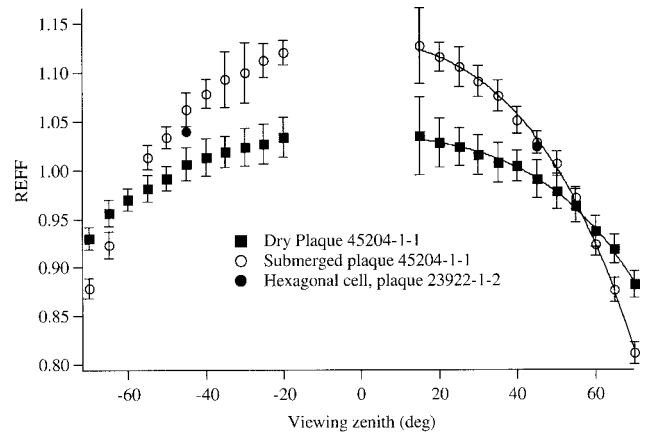


Fig. 1. REFFs of plaque 45204-1-1, dry and submerged in water, at normal illumination. Error bars are the standard deviation between the 24 individual measurements. Solid lines are the fit to Eqs. (10) and (11). Filled circles are the measurements of plaque (serial no. 23922-1-2) in the hexagonal cell as described in the text.

$$\text{REFF}^{\text{bare}} = \frac{L^{\text{bare}}}{\cos(\theta_v)} f(45^\circ), \quad (6)$$

where $f(45^\circ)$ is a normalization factor (in $\text{m}^2 \text{sr W}^{-1}$) that brings the $\text{REFF}(\theta_i = 0^\circ, \theta_v = 45^\circ)$ to a widely accepted value. By the reciprocity principle,⁵ this constant may be taken to be 0.99 from the value of the $\text{REFF}(\theta_i = 45^\circ, \theta_v = 0^\circ)$ at the 633 nm wavelength reported in the literature.^{2,7}

With the help of Eqs. (1), (2), and (6), one may derive the submerged REFF in two ways from Eqs. (3)–(5):

$$\text{REFF}_1^{\text{sub}} = \frac{L^{\text{sub}}}{L^{\text{jar}}} \frac{n}{T_{\text{abs}}(t_{\text{gw}}/t_{\text{ag}})^2} \text{REFF}^{\text{bare}}, \quad (7)$$

$$\text{REFF}_2^{\text{sub}} = \frac{n}{T_{\text{abs}}(t_{\text{ag}} t_{\text{gw}})^2} \frac{L^{\text{sub}}}{\cos(\theta_v)} f(45^\circ). \quad (8)$$

Equations (7) and (8) should be identical if the glass jar is perfectly optically smooth and hence the relationship

$$L^{\text{jar}} = L^{\text{bare}} t_{\text{ag}}^4 \quad (9)$$

holds strictly. Unfortunately, our glass jar had imperfections on its surfaces, and thus, although Eq. (9) holds approximately, large deviations of up to several percent were found at specific viewing angles (specific angles are relative to jar orientation). To overcome this problem and others that caused measurement uncertainties, we chose several orientations for which the effect of the imperfections was minimized. At each of these orientations the plaque was also rotated to minimize any orientation bias. These rotations at several jar orientations were averaged, and an average of Eqs. (7) and (8) was used to represent REFF^{sub} .

Figure 1 shows the final results for both dry and submerged REFF of plaque 45204-1-1. This is the

result of an average of 24 sets of measurements. The larger deviation at the 15° viewing angle is because at this position, the laser spot incident on the glass jar may at least partly enter into the field of view. The refractive indices used were 1.33 for pure water and 1.48 for pyroglass, giving $t_{\text{ag}} = 0.96$ and $t_{\text{gw}} \approx 1.0$. For the pure water used in this work, the absorption coefficient 0.30 m^{-1} at $0.633 \text{ }\mu\text{m}$ (Ref. 8) is assumed, leading to $T_{\text{abs}} = 0.94$. There are two main features in the REFF^{sub} as compared to $\text{REFF}^{\text{bare}}$. The first is that the REFF^{sub} has a steeper falloff than the corresponding dry (bare) plaque, meaning that the Spectralon plaque becomes more non-Lambertian when underwater. The second is that REFF^{sub} is brighter than $\text{REFF}^{\text{bare}}$ below the 55° viewing angle. Although REFF^{sub} is nearly 10% higher than $\text{REFF}^{\text{bare}}$ at near-normal viewing angles, the calculated albedo is 0.99 ± 0.01 and hence is still physically plausible. To test our results we placed a similar Spectralon plaque (serial no. 23922-1-2) into a quartz cuvette to measure both REFF^{jar} and REFF^{sub} . This cuvette was hexagonal, with a flat front window allowing the incident beam to enter normal to the surface and two adjacent windows at $\pm 45^\circ$ angles with respect to the front surface. In this case each of the two viewing directions at $\pm 45^\circ$ are viewed through a flat surface instead of a cylindrical one, and hence the radiance change from air to water becomes n^2 (see Appendix A) instead of n in Eqs. (7) and (8); the refractive index of fused quartz is 1.46. The result is appended to Fig. 1 as the solid circle mark, and it is seen to agree with the glass jar measurement within the measurement uncertainties.

Both the dry and the submerged REFF in the viewing angle range 15°–70° have been fit to three-term polynomials and the results are (with the fitting errors in parenthesis):

$$\text{REFF}^{\text{bare}} = 1.04(\pm 0.00) - 1.52(\pm 0.23) \times 10^{-5}\theta_r^2 - 3.14(\pm 0.45) \times 10^{-9}\theta_r^4, \quad (10)$$

$$\text{REFF}^{\text{sub}} = 1.13(\pm 0.00) - 3.85(\pm 0.28) \times 10^{-5}\theta_r^2 - 5.34(\pm 0.55) \times 10^{-9}\theta_r^4, \quad (11)$$

where θ_r is in degrees. We used this type of polynomial to avoid an artificial peak in the fit centered at near-normal angular positions. It should be pointed out that due to measurement uncertainties present in the gonio system, there were differences between the fit in the range 15°–70° and –70°–70°, and such differences reached their maxima at $\pm 70^\circ$ viewing angles (2.7% for dry and 4% for submerged, respectively). The larger uncertainty at larger angles was caused by the measurement geometry that had the flux collected by the detector falling by $\cos(\theta_v)$ since we illuminated a smaller area than we viewed.

3. Discussion

For many porous surfaces a particulate layer will appear darker when the interstitial pores are filled with water instead of air.^{9–11} This effect has been

attributed to forward scattering enhancement⁹ or total reflection-induced extinction occurring at the air–water interface.^{10,11} However, the effect we are seeing, the increased brightness at small viewing angles when the surface is submerged, is similar to the immersion effect seen when plastic diffusers are placed in the water.¹² In our case when light has entered the bulk Spectralon material, a decrease in the reflectance coefficient between the bulk Spectralon and the water will allow more light to escape the bulk material and enter the water medium again. It is likely this also causes the change in the shape of the REFF as radiance that has reflected back into the medium is not available to be backscattered into the Spectralon and then re-emitted at larger angles. Overall the albedo of the surface does not change significantly, from 0.97 ± 0.01 (dry) to 0.99 ± 0.01 (submerged).

Our selection of the value of the dry Spectralon $\text{REFF}(\theta_i = 0^\circ, \theta_v = 45^\circ)$ of 0.99 is supported by the literature. Other slightly higher values have been proposed such as 1.02.³ It is interesting to note that these values would be a multiplicative factor on all of our results. Including the dry and submerged albedos. This would lead to a dry albedo of 1.00 ± 0.01 and a submerged albedo of 1.02 ± 0.01 , which is clearly not physical. Hence we feel the value of 0.99 is reasonable.

Although there has been an attempt to model the BRDF of the Spectralon plaque by using a radiative transfer model with Henyey–Greenstein single-scattering phase function¹³; such a semiempirical approach may not be able to account for effects such as close packing, enhanced backscattering and underwater conditions in the BRDF. Thus direct measurement of the Spectralon BRDF is required.

Appendix A. Radiance Conservation for a Cylindrical Interface

The n^2 law of radiance propagating from air to water for a plane interface was derived explicitly in Ref. 14. Here we demonstrate that for a cylindrical interface the radiance change is n .

Figure 2 shows the schematics of the cylindrical water–air interface. In our case, medium 2 is the water in the cylindrical jar, while medium 1 is air. For simplicity, we will omit the glass wall refraction effect. The radiances of the rays in air and in water may be expressed, respectively, as

$$L_1 = \frac{\Delta\Phi_1}{\Delta A_1 \Delta\Omega_1},$$

$$L_2 = \frac{\Delta\Phi_2}{\Delta A_2 \Delta\Omega_2},$$

where $\Delta\Phi_1$ and $\Delta\Phi_2$ are the radiant powers in air and water, ΔA_1 and ΔA_2 are the cross-sectional areas of the rays, and $\Delta\Omega$ the solid angle. In cylindrical geometry, ΔA_1 and ΔA_2 are equal as long as the radiance propagates along the radial direction (perpendicular

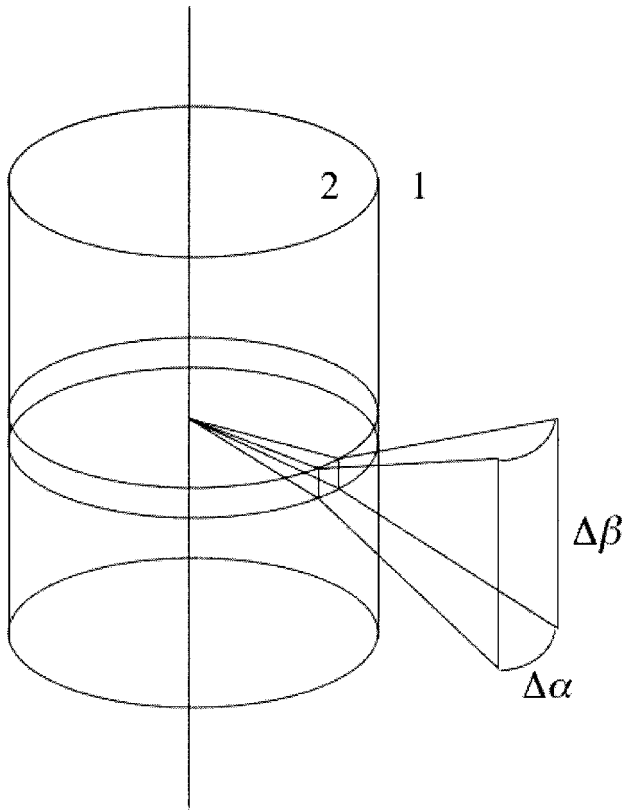


Fig. 2. Geometry of the radiance crossing a cylindrical interface between water (2) and air (1). Note that Snell's law applies only to β direction.

to the interface); the solid angles for the two rays are

$$\Delta\Omega_1 = \Delta\alpha_1\Delta\beta_1,$$

$$\Delta\Omega_2 = \Delta\alpha_2\Delta\beta_2,$$

respectively. Since the refraction occurs only along the β direction, we have (in the small angle limit)

$$\Delta\alpha_1 = \Delta\alpha_2,$$

$$n_1\Delta\beta_1 = n_2\Delta\beta_2.$$

Thus the ratio of the radiance in water to that in air is

$$\frac{L_2}{L_1} = \frac{\Delta\Phi_2 n_2}{\Delta\Phi_1 n_1}.$$

Taking the Fresnel transmittance $\Delta\Phi_2/\Delta\Phi_1$ to be 1 for simplicity, we have

$$\frac{L_2}{L_1} = \frac{n_2}{n_1}.$$

Similarly, for a spherical interface (a dome window, for example) if the ray is travelling in the radial direction, there should be no change of radiance at all.

We thank Albert Chapin for help in building the instrumentation used in this work. This work was supported by the Office of Naval Research Ocean Optics Program.

References

1. K. J. Voss, A. L. Chapin, M. Monti, and H. Zhang, "Instrument to measure the bidirectional reflectance distribution function of surfaces," *Appl. Opt.* **39**, 6197–6206 (2000).
2. C. Bruegge, N. Chrien, and D. Haner, "A Spectralon BRF data base for MISR calibration applications," *Remote Sens. Environ.* **76**, 354–366 (2001).
3. G. Meister, P. Abel, K. Carder, A. Chapin, D. Clark, J. Cooper, C. Davis, D. English, G. Fargion, M. Feinholz, R. Frouin, F. Hoge, D. Korwan, G. Lazin, C. McClain, S. McLean, D. Menzies, A. Poteau, J. Robertson, J. Sherman, K. Voss, and J. Yungel, "The second SIMBIOS radiometric intercomparison (SIMRIC-2), March–November 2002," (NASA/TM-2002-210006, 2003), Vol. 2.
4. H. Zhang and K. J. Voss, "Comparisons of bidirectional reflectance measurements and radiative transfer models," *Appl. Opt.* **44**, 597–610 (2005).
5. B. Hapke, *Theory of Reflectance and Emittance Spectroscopy* (Cambridge U. Press, 1993).
6. J. W. Giles and K. J. Voss, "Submerged reflectance measurements as a function of visible wavelength," in *Underwater Imaging, Photography, and Visibility*, R. W. Spinrad, ed., *Proc. SPIE* **1537**, 140–146 (1991).
7. X. Feng, J. R. Schott, and T. Gallagher, "Comparison of methods for generation of absolute reflectance-factor values for bidirectional reflectance-distribution function studies," *Appl. Opt.* **32**, 1234–1242 (1993).
8. R. M. Pope and E. S. Fry, "Absorption spectrum (380–700 nm) of pure water. II. Integrating cavity measurements," *Appl. Opt.* **36**, 8710–8723 (1997).
9. S. A. Twomey, C. F. Bohren, and J. L. Mergenthaler, "Reflectance and albedo differences between wet and dry surfaces," *Appl. Opt.* **25**, 431–437 (1986).
10. A. Angstrom, "The albedo of various surfaces of ground," *Geogr. Ann.* **7**, 323–342 (1925).
11. J. Lekner and M. C. Dorf, "Why some things are darker when wet," *Appl. Opt.* **27**, 1278–1280 (1988).
12. J. Tyler and R. Smith, *Measurements of Spectral Irradiance Underwater* (Gordon and Breach, 1970), p. 102.
13. G. B. Courreges-Lacoste, J. G. Schaarsberg, R. Sprik, and S. Delwart, "Modeling of Spectralon diffusers for radiometric calibration in remote sensing," *Opt. Eng.* **42**, 3600–3607 (2003).
14. C. D. Mobley, *Light and Water-Radiative Transfer in Natural Waters* (Academic, 1994), p. 159.